An 8x4 Continuous Transverse Stub Array fed by Coaxial Ports

Siyi Zhou, Mauro Ettorre, Anthony Grbic

An 8×4 Continuous Transverse Stub Array fed by Coaxial Ports

Siyi Zhou, Mauro Ettorre, *Senior Member, IEEE*, and Anthony Grbic, *Fellow, IEEE*

***Abstract*—Continuous transverse stub arrays are wide band, wide scanning antennas consisting of an arrangement of long slots or parallel plate waveguide apertures radiating in free space. A line source is generally required to feed these arrays. Here, we show that such a line source can be created over the radiating aperture using a 2D arrangement of coaxial probe transitions. The coaxial transitions are directly integrated into the parallel plate waveguides feeding the slots. Such a solution avoids using quasi-optical systems or bulky corporate networks to feed the array. The proposed 2D feeding scheme also allows steering the main beam of the array. This is an additional benefit with respect to previous designs for which scanning was limited to a single plane. An array of 8×4 elements validates the concept at 5.8 GHz. Measurements show that the array exhibits a field of view of $\pm 30^\circ$ in elevation over the $5.4-6.2$ GHz band, with an active reflection coefficient for the central elements better than -10 dB.**

***Index Terms*—Continuous transverse stub, slot arrays, wide band antennas.**

I. Introduction

THE continuous transverse stub (CTS) array is an established solution for wide band and wide scanning Satcom antenna applications [1]-[5]. The basic radiating element is a non-resonant, long slot or broad stub fed by a parallel plate waveguide (PPW) network. An array of such elements can be fed either in series or in parallel. Both feeding architectures require a line source to properly illuminate the array. The line source can be realized using a quasi-optical system [5] or by integrating active components within the PPW feeding network [6], [7]. Generally, quasi-optical systems are used in combination with a corporate feed system. Such a solution preserves the large bandwidth behaviour of CTS arrays, but limits the scanning ability of the array to a plane parallel to the radiating slots [5].

Here, we use coaxial probe transitions to feed a CTS array. The coaxial transitions are directly integrated into the PPW lines feeding each radiating slot to generate the required line source. In this way, each slot is fed in parallel, as in a corporate network while preserving the compactness of the structure. The proposed feeding system also offers the possibility to steer the main beam of the array in any direction in free space once the required phase and amplitude excitations are provided at the input ports of the coaxial probes.

The design of an array of four slots, each fed by eight coaxial probes (8×4 input ports), is proposed to validate the concept at an operating frequency of 5.8 GHz. The active reflection coefficient of the array's unit cell is evaluated in an infinite array environment for scanning over the principal planes of the array. Each unit cell of the array is fed by a coaxial transition, which allows scanning range $\pm 30^\circ$ in elevation from 4.8 GHz to 6.2 GHz. This corresponds to a fractional bandwidth of 24% around 5.8 GHz. A prototype of the array is manufactured from aluminum using a standard milling process. The measured active reflection coefficient of the central elements of the finite array is compared to full-wave simulations, and to the infinite case validating the design and general conclusions. Measured radiation patterns are also validated through full-wave simulations. Measurements demonstrate that the antenna can steer its main beam in the both principal, and diagonal planes over a field of view of $\pm 30^\circ$, while maintaining cross-polarization levels below over -20 dB.

The paper is organized as follows. Section II presents the design of the unit cell of the array fed by coaxial transitions. The active reflection coefficient of the unit cell is provided for scanning angles up to 30°. The prototype and the measured active reflection coefficient and radiation patterns are discussed in Section III. Finally conclusions are drawn in Section IV.

II. Antenna design

The architecture of the 8×4 CTS array fed by coaxial probes is shown in Fig. 1a. Each of the four slots comprising the array is fed by eight coaxial ports through air-filled PPW lines. The unit cell of the array, with a coaxial probe transition, is highlighted in Fig. 1a. Side views of the unit cell in the xz- and yz-planes are also provided in Fig. 1b. The design of the radiating slots of the array follows the procedure outlined in [3]. The slot width, w_s, and height of the feeding PPW lines are chosen to only allow the propagation of the Transverse Electromagnetic (TEM) mode of the PPW lines at the arrays's upper frequency of operation. The slot width w_s and periodicity d_y are designed to yield an active reflection coefficient over the slot plane (reference plane R1 in Fig. 1b) lower than -10 dB for the operating band and scanning range. A two step quarter-wave impedance transformer is then used to match the active impedance of the slot to the input PPW line (reference plane R2 in Fig. 1b) where the coaxial probe transition is located. The input PPW line is then matched to the 50 Ohm impedance of the coaxial transition using a back short and a cylindrical intrusion within the PPW [8] (refer to Fig. 1b for geometrical details). In particular, the cylindrical intrusion within the PPW and a rectangular cavity around the connection of the probe transition (refer to Fig. 1b) are employed to match over the band of interest. Full-wave simulations in an infinite array environment are used to derive the final geometrical dimensions of the unit cell as provided in Fig. 1. The periodicity along the x-axis (d_x) of the coaxial input ports is set to less than a half wavelength at the upper frequency of operation to avoid grating lobes. Specifically d_x is chosen equal to $d_y = 24$ mm. Note that the antenna is linearly polarized with the electric field of the feeding TEM mode oriented along the y-axis. The E- and H-plane correspond to the yz-plane and xz-plane in Fig. 1.

Manuscript received XX/XX/2018; revised XX/XX/2018.

This work was supported in part by the French National Research Agency (ANR) under grant n°ANR-14-CE26-0030-01, the UM-KACST Joint Center for Microwave Sensor Technology, the European Union through the European Regional Development Fund (ERDF), and the French region of Brittany, Ministry of Higher Education and Research, Rennes Métropole and Conseil Départemental 35, through the CPER Project SOPHIE / STIC & Ondes.

S. Zhou and M. Ettorre are with the Institut d'Electronique et de Télécommunications de Rennes (IETR), UMR CNRS 6164, Université de de Rennes 1, Rennes Cedex 35042, France (e-mail: siyi.zhou, mauro.ettorre@univ-rennes1.fr).

A. Grbic is with the Radiation Laboratory, Department of Electrical Engineering and Computer Science, University of Michigan, Ann Arbor, MI 48109-2122 USA, and also with the Center of Photonic and Multiscale Materials, University of Michigan, Ann Arbor, MI 48109-2122 USA (e-mail: agrbic@umich.edu).

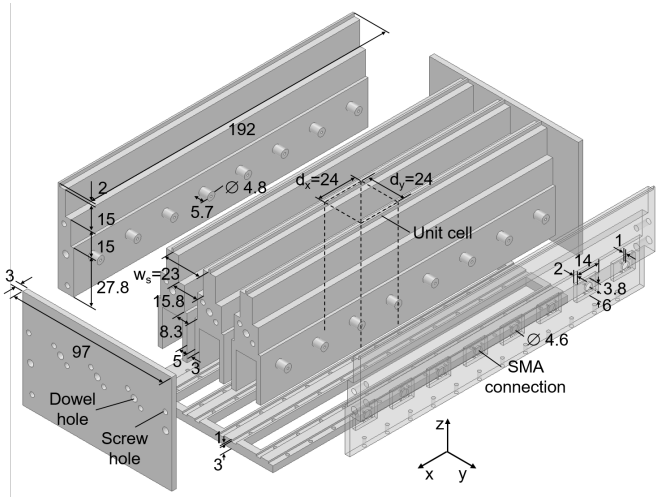

(a)

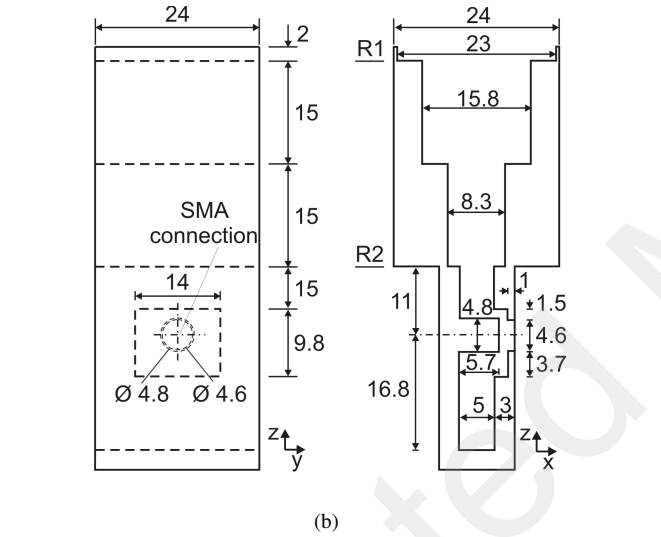

(b)

Fig. 1. The 8×4 CTS array. (a) Perspective view. The unit cell of the array is outlined by a dashed box. (b) Side view of the unit cell of the array along the yz- and xz-planes. The dimensions are in mm.

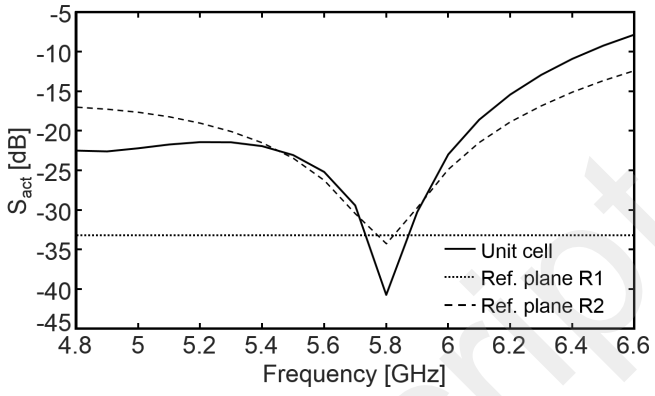

(a)

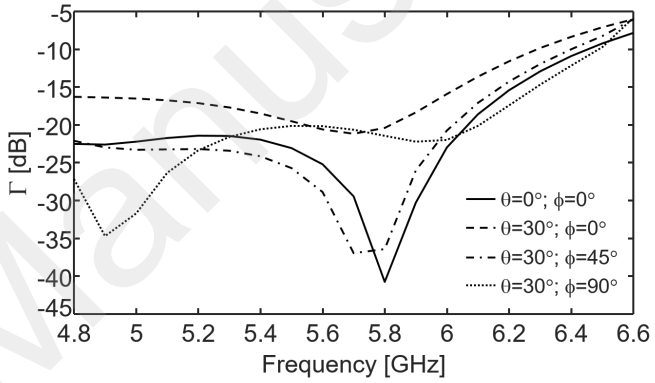

(b)

Fig. 2. Active reflection coefficient of a unit cell of the array in an infinite periodic environment. (a) At the reference planes R1 and R2 in Fig. 1 for broadside radiation. (b) At the SMA connection for different scanning angles and planes of observation.

The bandwidth, frequency of operation and scanning range specification for the design are chosen based on possibly using the array as a Van Atta mirror in a far-field wireless power transfer system [9], [10]. In particular, the goal was an active reflection coefficient lower than -10 dB over the $5.4-6.2$ GHz band, for a scanning range in elevation of $\pm 30^{\circ}$.

Fig. 2a provides the active reflection coefficient of the unit cell from 4.8 to 6.2 GHz at the reference planes R1, R2 and at the SMA connection for broadside direction. The wide band behaviour of the radiating slot at the reference plane R1 is highlighted by a flat active reflection coefficient in the entire band. As expected, the two step-quarter-wave transformers introduces a resonance at the design frequency of 5.8 GHz, but does not affect the wide band behaviour of the unit cell. The same behaviour is observed at the SMA connection after the coaxial probe transition. In addition, Fig. 2b plots the active reflection coefficient of the unit cell from 4.8 to 6.2 GHz along the E-, D-(diagonal plane, $\phi = 45^{\circ}$ in Fig. 1) and H-plane at broadside $\theta = 0^{\circ}$ and $\theta = 30^{\circ}$. The unit cell is matched over the considered band (24% relative bandwidth around 5.8 GHz) and scanning range. Note that the coaxial transition allows 2D scanning (refer to Section III) and does not require a corporate feed network or quasi-optical system, as in [5]. It is worth mentioning that connected arrays can provide a similar performance [11]-[13].

III. Prototype and Measurements

The array prototype is shown in Fig. 3. It is made of various aluminium parts fabricated using a computer numerical control (CNC) milling machine, and assembled as outlined in [5]. The assembly uses dowel pins and screws with an expected alignment accuracy better than 50μm. The 32 SMA connectors used for the input ports of the array are visible in Fig. 3a. During measurements, coaxial cables were attached to the SMA connectors to ease access to the input ports of the array. The cables were not considered in the full-wave simulations of the array.

The scattering matrix (32×32 elements) of the array was measured. The active reflection coefficient at each input port of the array was then derived by assuming a uniform illumination and the required phase profile for scanning [14]. The active reflection coefficient for

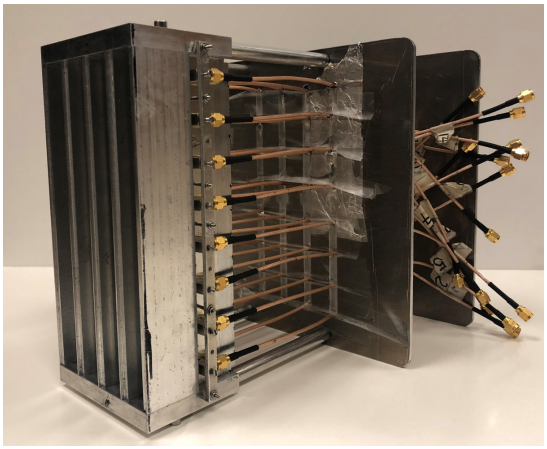

(a)

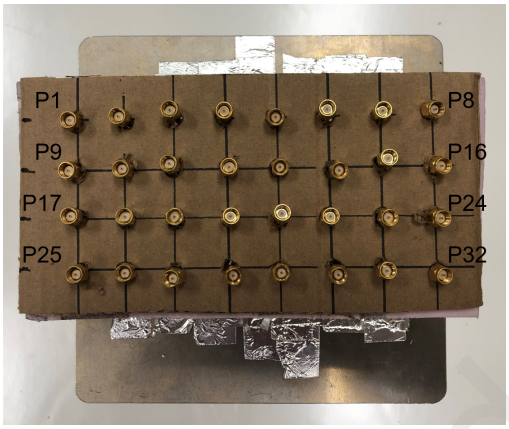

(b)

Fig. 3. Prototype. (a) Perspective view. (b) Rear view showing the labelled input ports. The coaxial cables and mechanical support used for measurement are visible in the photograph.

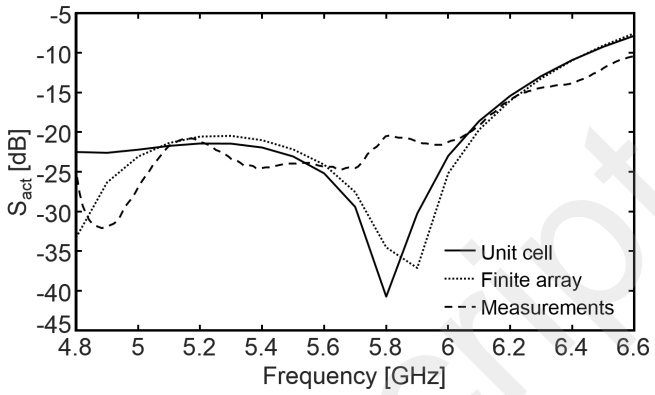

(a)

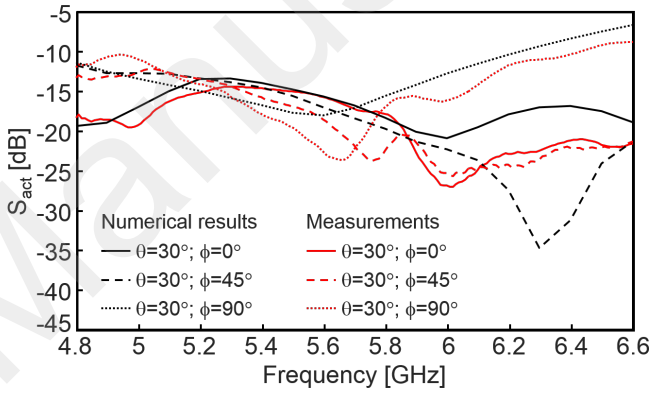

(b)

Fig. 4. Active reflection coefficient of the central element of the array (P12 in Fig. 3b). (a) Broadside radiation. (b) Scanning in E-, D- and H-plane at $\theta = 30°$. The active reflection coefficient of the unit cell for broadside radiation in an infinite array environment is shown for comparison.

the central element of the array (Port 12 in Fig. 3b) is shown in Fig. 4a for a broadside excitation. Full-wave simulations of the finite and infinite array are also reported for comparison. The measured active reflection coefficient is in line with the infinite and finite array numerical results. Please note that de-embedding was performed on the measured results to remove the impact of the cables on the active reflection coefficients. The measured active reflection coefficient for the central element for scanning at $\theta = 30°$ in elevation is reported in Fig. 4b along the E-, D- and H-planes. The simulated active reflection coefficient for the central element of the array is provided for comparison in the considered scanning directions. The central element is matched over the design band $5.4 - 6.2$ GHz and even beyond. It is worth mentioning that similar results were achieved for all other input ports, except for the most external ones as Port1 (see Fig. 3b). This is expected for such a small array. Different aperture illuminations may be used to improve the matching of the external elements of the array.

The 3D embedded element patterns corresponding to each input port of the array were measured in the anechoic chamber at IETR by feeding the considered port and terminating all other ports with

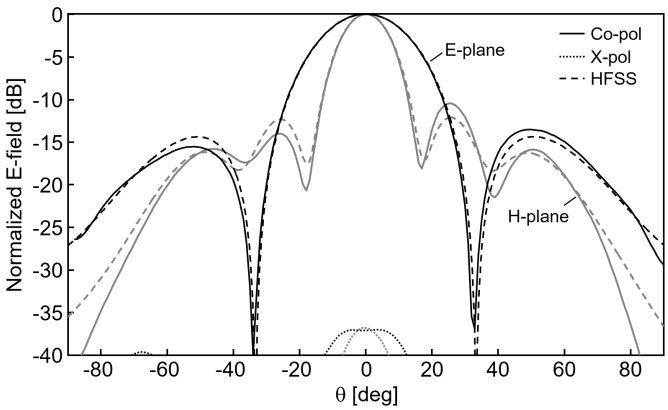

Fig. 5. Normalized radiation patterns of the array for a uniform illumination along the E and H-plane for broadside radiation at 5.8 GHz.

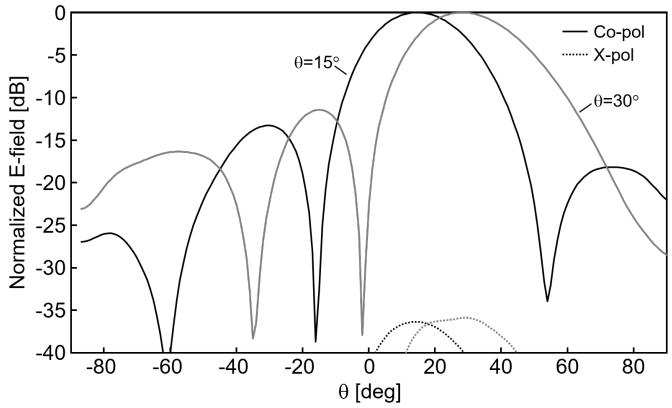

(a)

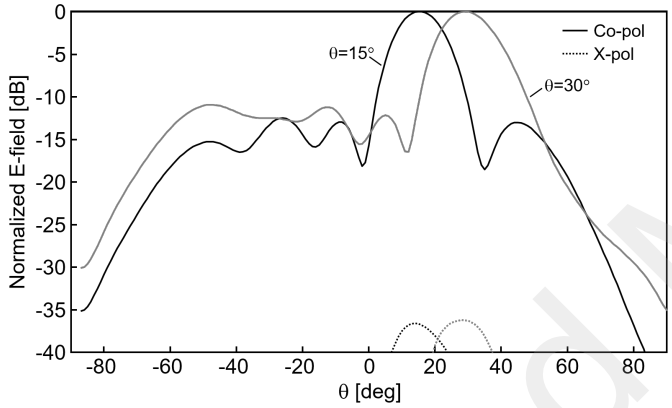

(b)

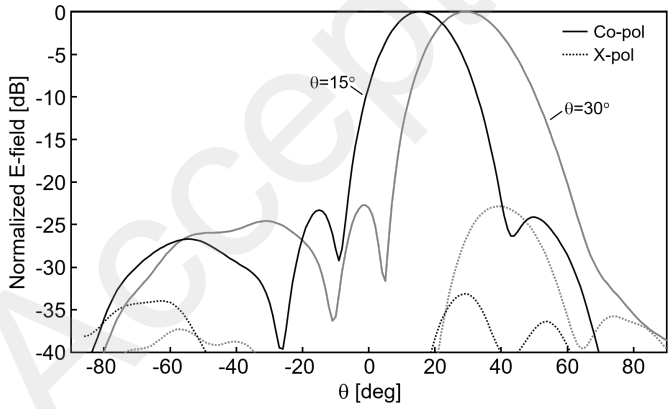

(c)

Fig. 6. Normalized radiation patterns of the array for a uniform illumination and different scan angles at 5.8 GHz. (a) E-plane. (b) H-plane. (b) D-plane.

matched loads. The radiation patterns of the full array were then retrieved in the E-, H- and D-planes by post-processing the embedded element patterns and applying the require phase gradient for scanning. The final radiation patterns of the array assuming uniform illumination are shown in Fig. 5 at 5.8 GHz along the E-, H-plane for broadside direction. Good agreement is observed between simulation and measurement.

The measured radiation patterns along the E-, H- and D-planes at 5.8 GHz are shown Fig. 6 for two different scan angles. The radiation patterns have been normalized to their maximum. The 2D scanning ability of the array is validated for the CTS array. The 2D scanning ability is enabled by the proposed coaxial probe transition and antenna architecture. The proposed array also exhibits low cross-polarization levels (< -20 dB) in all planes and for all the considered scanning angles [15]. These results confirm the polarization purity of the radiated field. Similar measured results, in terms of scanning, are obtained in the band $5.4-6.2$ GHz and not reported here for brevity.

The measured realized gain and directivity of the array for a uniform illumination are estimated equal to 18.6 dBi and 17.8 dB, respectively, at broadside at 5.8 GHz. The total loss of the antenna is equal to 0.8 dB. This includes the metallic, cable and transition losses. The major contribution to the losses is attributed to the cables which are 30.48 cm long with losses on the order of 0.6 dB.

IV. Conclusion

An 8×4 continuous transverse stub array fed by coaxial probes has been presented. Each slot of the array is fed by eight equally-spaced coaxial probes in the PPW lines feeding the slots. The proposed feeding scheme allows 2D steering of the antenna main beam in free space. Such a solution overcomes the limitations of earlier CTS designs which achieve scanning only in one plane, at a given frequency of operation. In addition, the proposed scheme does not require a quasi-optical system nor active components within the corporate feed network of the array, easing the fabrication. A prototype made of aluminum using CNC milling has been presented and validated through full-wave simulations and measurements. The active reflection coefficient of the array is less than -10 dB over the band $5.4 - 6.2$ GHz for scanning up to 30° in elevation. Measurements show that the antenna can steer its main beam over the considered range with cross-polarization levels below -20 dB. The proposed antenna may be a good candidate for applications requiring a wide band, wide scanning antenna. The proposed antenna could be used as a Van Atta mirror for far field wireless power transfer applications.

References

[1] W. W. Milroy, "Continuous transverse stub element devices and methods of making same," United States Patent 5 266 961, Nov. 30, 1993.

[2] W. W. Milroy, "Compact, ultra-wideband, antenna feed architecture comprising a multistage, multilevel network of constant reflection-coefficient components," United States Patent 6 075 494, June 13, 2000.

[3] F. Foglia Manzillo, M. Ettorre, M. Casaletti, N. Capet, and R. Sauleau, "Active impedance of infinite parallel-fed continuous transverse stub arrays," *IEEE Trans. Antennas Propag.*, Vol. 63, No. 7, pp. 3291 - 3297, July 2015.

[4] F. Foglia Manzillo, M. Ettorre, M. S. Lahti, K. T. Kautio, D. Lelaidier, E. Seguenot, and R. Sauleau, "A multilayer LTCC solution for integrating 5G access point antenna modules," *IEEE Trans. Microw. Theory Tech.*, Vol. 64, No. 7, pp. 2272 - 2283, July 2016.

[5] M. Ettorre, F. Foglia Manzillo, M. Casaletti, R. Sauleau, L. Le Coq, and N. Capet, "Continuous transverse stub array for Ka-band applications," *IEEE Trans. Antennas Propag.*, Vol. 63, No. 11, pp. 4792 - 4800, Nov. 2015.

[6] R. S. Robertson, W. H. Henderson, R. T. Lewis, and R. J. Broas, "Transverse device array radiator ESA," United States Patent 7 106 265, Sep. 12, 2006.

[7] J. J. Lee, S. R. Wilkinson, R. A. Rosen, K. V. Krikorian, and I. L. Newberg, "MMW electronically scanned antenna," United States Patent 7 061 443, Jun. 13, 2006.
[8] D. M. Pozar, *Microwave engineering*, 4nd ed., John Wiley & Sons, Inc., New York, 2012.
[9] M. Ettorre, W. A. Alomar, and A. Grbic, "Radiative wireless power transfer system using wideband, wideangle slot arrays," *IEEE Trans. Antennas Propag.*, Vol. 65, No. 6, pp. 2975 - 2982, June 2017.
[10] M. Ettorre, W. A. Alomar, and A. Grbic, "2D Van Atta array of wideband, wideangle slots for radiative wireless power transfer systems," *IEEE Trans. Antennas Propag.*, Vol. 66, No. 9, pp. 4577 - 4585, Sept. 2018.
[11] D. Cavallo, W. H. Syed, and A. Neto, "Connected-slot array with artificial dielectrics: a 6 to 15 GHz dual-pol wide-scan prototype," *IEEE Trans. Antennas Propag.*, Vol. 66, No. 6, pp. 3201 - 3206, June 2018.
[12] D. Cavallo, A. Neto, G. Gerini, A. Micco, and V. Galdi, "A 3- to 5-GHz wideband array of connected dipoles with low cross polarization and wide-scan capability," *IEEE Trans. Antennas Propag.*, Vol. 61, No. 3, pp. 1148 - 1154, Mar. 2013.
[13] E. Yetisir, N. Ghalichechian, and J. L. Volakis, "Ultrawideband array with 70° scanning using FSS superstrate," *IEEE Trans. Antennas Propag.*, Vol. 64, No. 10, pp. 4256 - 4265, Oct. 2016.
[14] D. M. Pozar, "The active element pattern," *IEEE Trans. Antennas Propag.*, Vol. 42, No. 8, pp. 1176 - 1178, Aug. 1994.
[15] A. C. Ludwig,, "The definition of cross polarization," *IEEE Trans. Antennas Propag.*, Vol. AP-21, No. 1, pp. 116 - 119, Jan. 1973.